

Supporting information

Thermoelectric properties of organic charge transfer salts from first-principle investigations: Role of molecular packing and triiodide anions

Yishan Wang,^{a, b} Meng zhao,^{a, b} Hu zhao,^c Shuzhou Li,^d Jia Zhu,^{*b, a} and Weihai Fang ^{*a}

^a College of Chemistry, Key Laboratory of Theoretical & Computational Photochemistry of Ministry of Education, Beijing Normal University, Beijing 100875, P. R. China .

^b Laboratory of Theoretical and Computational Nanoscience, CAS Center for Excellence in Nanoscience, National Center for Nanoscience and Technology, Chinese Academy of Sciences, 100190, Beijing, China.

^c Department of Physics, Beijing Normal University, Beijing 100875, P. R. China.

^d School of Materials Science and Engineering, Nanyang Technological University, 50 Nanyang Avenue, 639798 Singapore

Corresponding author. Email: zhujia@nanoctr.cn

fangwh@bnu.edu.cn

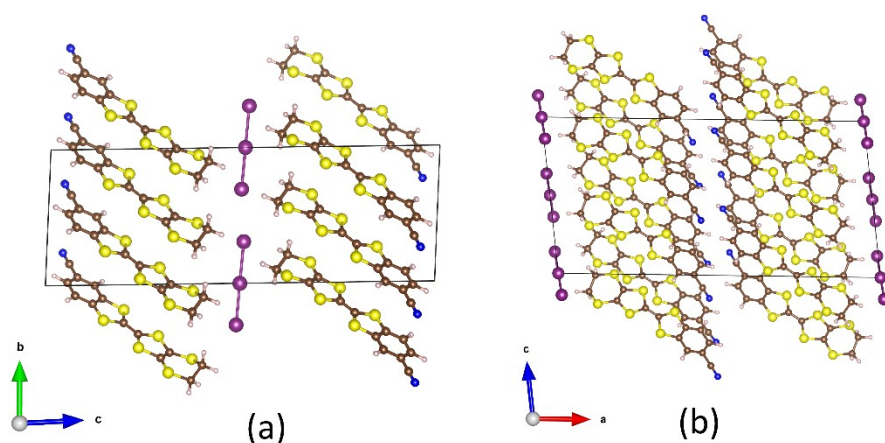


Figure S1. The new type of bilayer structure, where two layers of donor molecules stack with a head-to-head mode between triiodide anions via C-N \cdots H interaction along *c*-axis in (a) β'' -phase CT salt and along *a*-axis in (b) κ -phase CT salt, respectively.

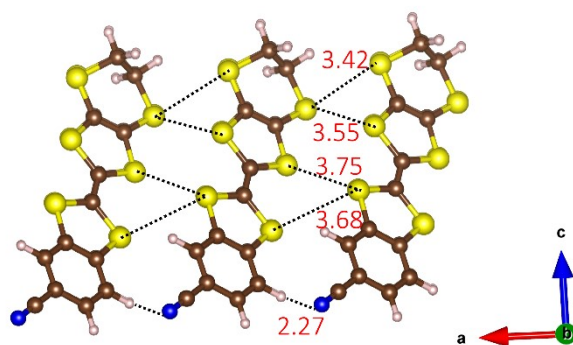


Figure S2. The denser inter-stack interaction networks consisting of S \cdots S and C-N \cdots H non-covalent interactions in β'' -phase CT salt. The unit of the values in the figure is angstrom \AA .

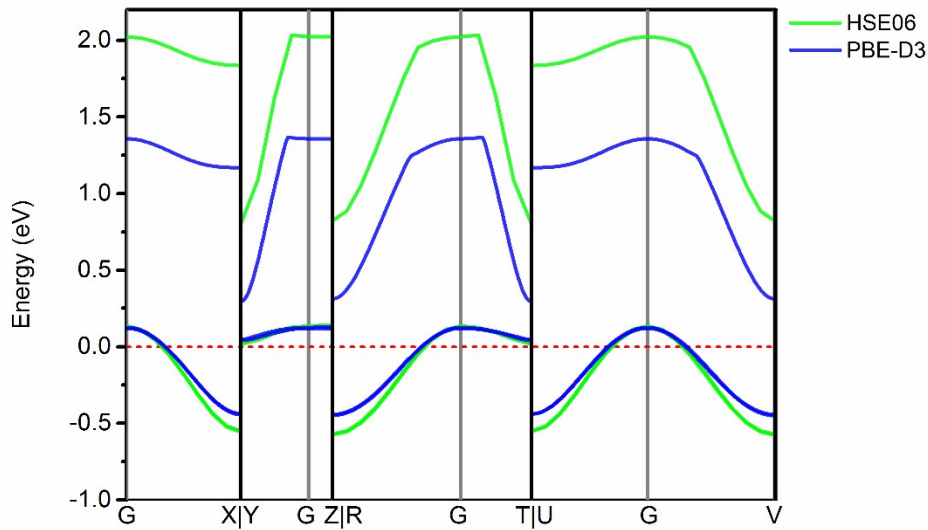


Figure S3. The valance band and conduction band of β'' -phase CT salt calculated by HSE06 functional compared with that calculated by PBE-D3 functional. The zero of energy is given at the Fermi energy. The p-type degenerate characteristic is confirmed by the HSE06 functional and the valance band profile are coincident with that of PBE-D3, especially the profile of the valance band that dominates the hole TE transport properties. Besides, the valance and conduction bands have similar width with those of PBE-D3. The band gap at HSE06 level is 0.663 eV, which is larger than the band gap calculated by PBE-D3 (0.164 eV).

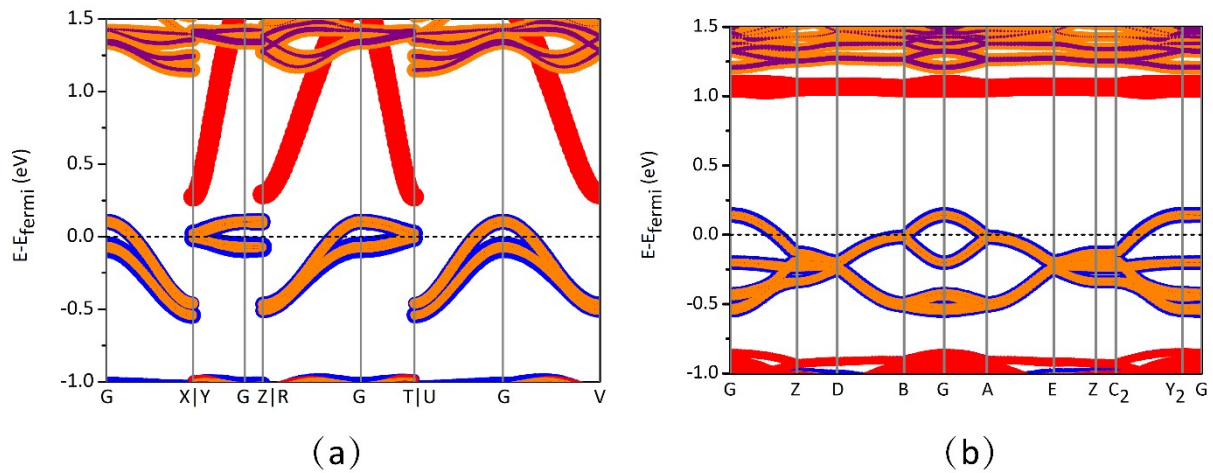


Figure S4. Elements-resolved band structures of (a) β'' -phase and (b) κ -phase CT salts. The bands projected onto C, S, N, and I element are highlighted in orange, blue, purple, and red respectively. The line width reflects the weight of each element to the band. The zero of energy is given at the Fermi energy.

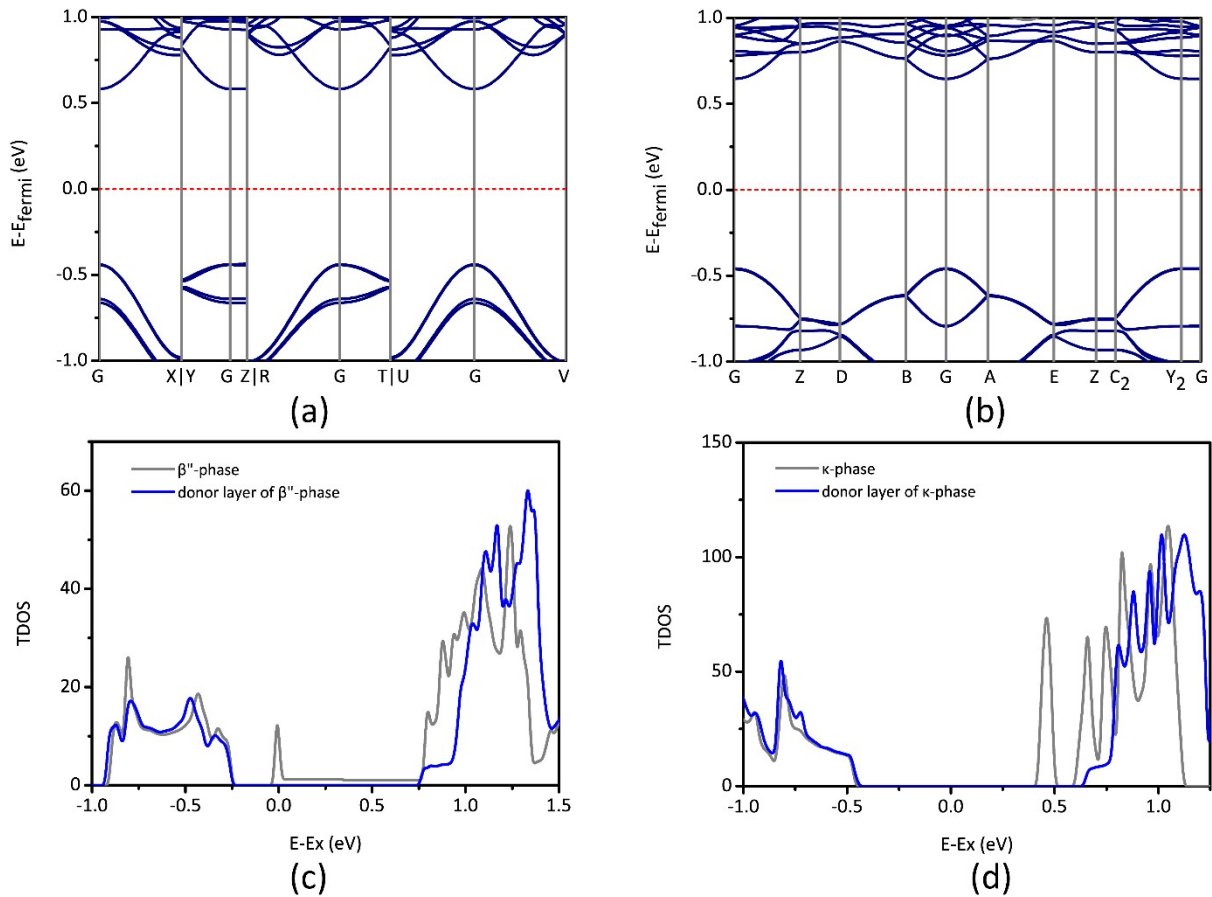


Figure S5. The band structures and total DOS (TDOS) of the donor layers for (a) (c) β'' -phase and (b) (d) κ -phase CT salts. The zero of energy is given at the Fermi energy. The high-symmetry k -points in the first Brillouin zone can be found at Figure 2. The TDOS of the β'' - and κ -phase CT salts, i.e., the crystal structures consisting of the donor and triiodide anions layers, are also shown represented by gray curve in (c) and (d) to compare with the TDOS of the donor layers (blue curve), i.e., the crystal structures that remove the triiodide anion layers.

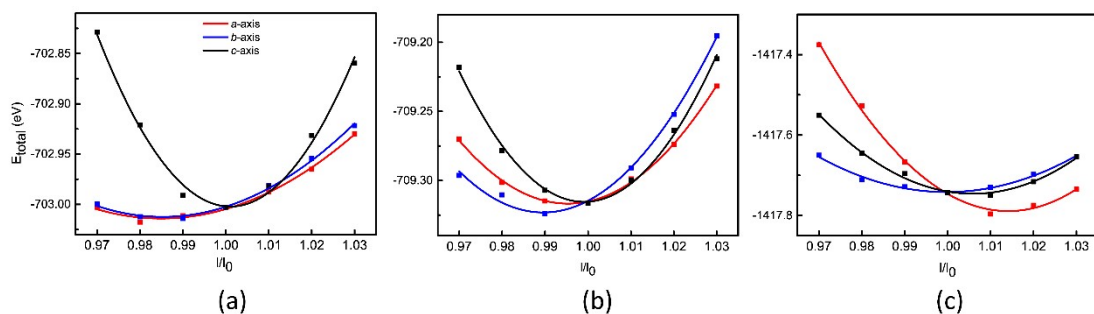


Figure S6. The parabola relations between the total energy E_{total} of the crystal and the deformation degree of the lattice l/l_0 for (a) pristine 5-CNB-EDT-TTF, (b) β'' -phase and (c) κ -phase (5-CNB-EDT-TTF)₄I₃ CT salts.

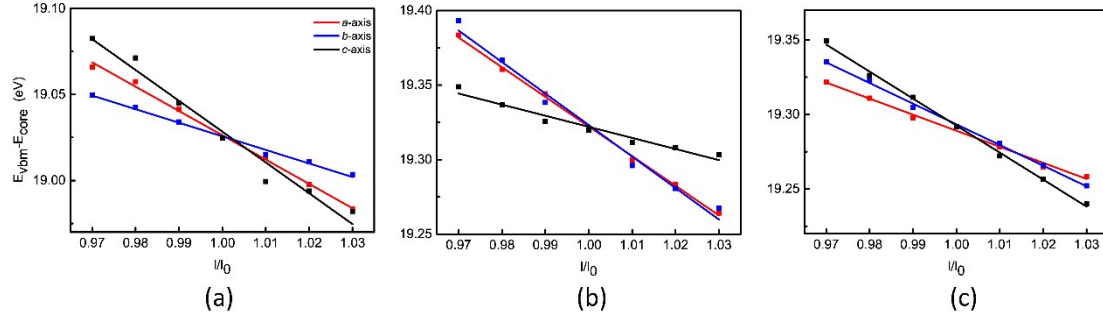


Figure S7. The linear relations between the band energy (or Fermi level) and the deformation degree of the lattice l/l_0 . The energies are VBM E_{VBM} for (a) pristine 5-CNB-EDT-TTF and the Fermi level E_{fermi} for (b) β'' -phase and (c) κ -phase (5-CNB-EDT-TTF) $_4I_3$ CT salts with respect to the core level E_{core} , respectively.

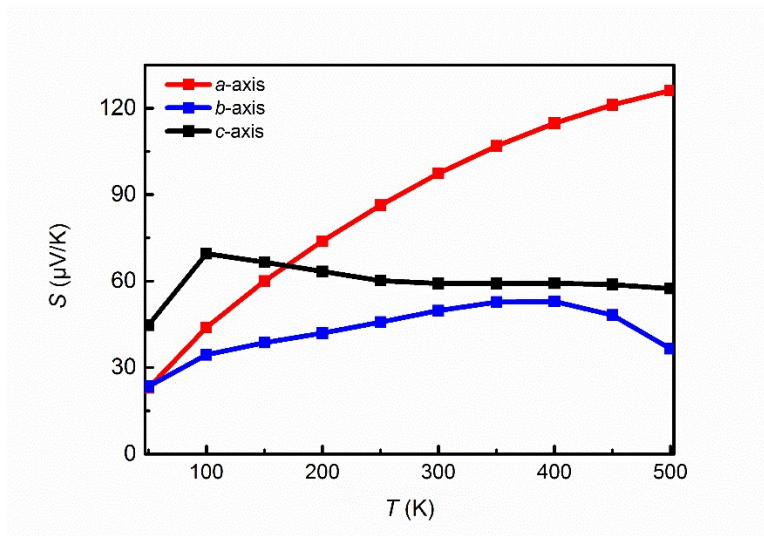


Figure S8. Temperature dependence of the Seebeck coefficient S for β'' -phase (5-CNB-EDT-TTF) $_4I_3$ CT salt in the range of 50 K to 500 K calculated with PBE-D3 functional. Due to the significant counteraction of negative contribution of S_{CB} , the nonmonotonic behavior is found along b - and c -axes.

Table S1. Calculated electrical conductivity σ , Seebeck coefficient S , and power factor PF of β'' -phase (5-CNB-EDT-TTF) $_4I_3$ CT salts along a -, b -, and c -axes at intrinsic region at RT, using the PBE-D3 band gap 0.164 eV and HSE06 band gap 0.663 eV, respectively.				
β'' -phase	axis	σ ($10^3 \Omega^{-1} \text{cm}^{-1}$)	S ($\mu\text{V/K}$)	PF ($\mu\text{Wcm}^{-1}\text{K}^{-2}$)
Band gap = 0.663 eV	a	7.688	98.3	74.29
	b	0.995	50.8	2.568
	c	0.040	60.2	0.241

The electrical conductivity, Seebeck coefficient, and power factor of β'' -phase CT salt using bandgap obtained by HSE06 functional are calculated as shown in Table S1. Almost identical values computed by HSE06 functional at the room temperature (RT) can be found compared with those computed by PBE-D3 functional.

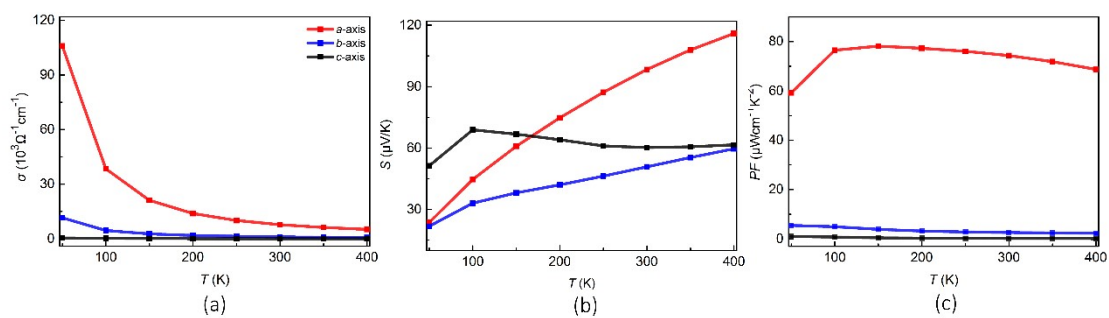


Figure S9. The temperature dependence of electrical conductivity, Seebeck coefficient, and power factor for β'' -phase $(5\text{-CNB-EDT-TTF})_4\text{I}_3$ CT salt calculated with bandgap obtained by HSE06 functional. The profiles obtained by bandgaps of HSE06 functional exhibit the similar trends as the temperature varies compared with those of PBE-D3 functional, which verifies the reliability of PBE-D3 functional in evaluating TE transport properties of CT salts.